Noninvasive Functional Imaging of Volumetric Cardiac Electrical Activity: A Human Study on Myocardial Infarction

Linwei Wang[1], Ken C.L. Wong[1], Heye Zhang[2], and Pengcheng Shi[1]

[1] Golisano College of Computing and Information Science
Rochester Institute of Technology, Rochester, NY, USA
maomaowlw@mail.rit.edu
[2] Bioengineering Institute, University of Auckland, Auckland, New Zealand

Abstract. Identification of infarct substrates provides necessary guidance to the prevention and treatment of cardiac arrhythmias. Compared to diagnostic criteria of body surface potentials (BSP) or electrophysiological information on heart surfaces, the underlying volumetric cardiac electrical activity is of more direct clinical relevance in exhibiting patient-specific arrhythmic dynamics and arrhythmogenic substrates. We have developed a paradigm for noninvasive imaging of volumetric myocardial transmembrane potential from BSPs. In this paper, we present a human study for a patient with acute myocardial infarction. Using patient MRI and BSP data, the framework is able to reconstruct details of the complete arrhythmic electrical activity on the 3D myocardium of the patient. Exploring a subset of the results, the extent, centroid and affected segments of the infarct is correctly evaluated, with comparable performance to existent best results. This human study demonstrates the potential of the presented paradigm as a noninvasive functional imaging technique for patient-specific volumetric cardiac electrical activity in practice.

1 Introduction

Arrhythmogenic substrates created by myocardial infarction (MI) lead to a high incidence of lethal ventricular tachycardia and fibrillation. Identification of infarct substrates could significantly improve the prevention and treatment of cardiac arrhythmias. The ablative therapy is a typical example requiring such guidance to destroy or interrupt arrhythmogenic substrates. In current clinical practice, the 12-lead ECG is the most frequently used tool for evaluating MI, though the limitaion in its diagnostic capability has been widely recognized [1].

As an extension to ECG, body surface potential map (BSPM) records potentials from hundreds of electrodes on thorax surface. It provides functional images implying the spatiotemporal dynamics of the underlying cardiac electrical activity. While large efforts have been put to build up BSPM database for arrhythmia identification [2], BSPM is not able to reflect local details of the electrical activity ongoing throughout the 3D myocardium, since each electrode actually only measures a *smoothed integration* of the entire cardiac activity.

D. Metaxas et al. (Eds.): MICCAI 2008, Part I, LNCS 5241, pp. 1042–1050, 2008.

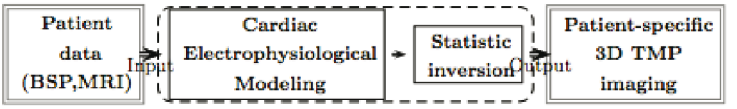

Fig. 1. Noninvasive functional imaging of volumetric cardiac electrical activity

The inverse problem of electrocardiography (IECG) aims at noninvasive reconstruction of cardiac electrical activity from BSPMs. Several recent IECG approaches have been applied to MI evaluation [3,4]. Mostly the solutions are confined to electrophysiological information on heart surfaces, assuming that it contains characteristics associated with infarct substrates [3]. However, to localize intramural arrhythmogenic substrates more directly, reconstruction of volumetric cardiac electrical activity is desired. A heart-model-based approach was reported in simulation experiments to estimate the site and size of MI in 3D myocardium [4]. By deterministically optimizing the heart model, it imposes high requirements on the initial approximation and modeling of the infarct. How these factors would affect the results in real-data experiments remains unknown.

We have presented a model-constrained Bayesian paradigm for noninvasive imaging of volumetric myocardial transmembrane potential (TMP) from BSPMs [5]. Its practical potential has been demonstrated by extensive phantom experiments in cardiac arrhythmia imaging [6]. In this paper, we experiment this paradigm for a human study. With MRI and BSP data collected from a patient with acute MI, volumetric arrhythmic TMP dynamics of this specific subject's heart is noninvasively imaged. The associated MI evaluation is compared to existent works and cardiologists' interpretation of the infarct. This study validates the potential of the paradigm as a noninvasive functional imaging technique for patient-specific volumetric cardiac electrical activity, and demonstrates how a subset of the results is of promising clinical relevance in MI evaluation.

2 Method

2.1 Model-Constrained Bayesian Paradigm for TMP Imaging

The architecture of this noninvasive TMP imaging paradigm is illustrated in Fig 1. To combine general physiological knowledge and patient clinical data with regard to their respective uncertainties, the Bayesian paradigm estimates patient-specific TMPs via statistic inversion. *A priori* physiological knowledge is contained in the cardiac electrophysiological system customized to patient heart-torso structure. It consists of volumetric myocardial TMP activity model for system dynamics and TMP-to-BSP model for system observations. After reformulating the physiological system into a stochastic state space representation with associated model and data errors, data assimilation is utilized to estimate volumetric myocardial TMP dynamics from BSPMs of specific patients [5].

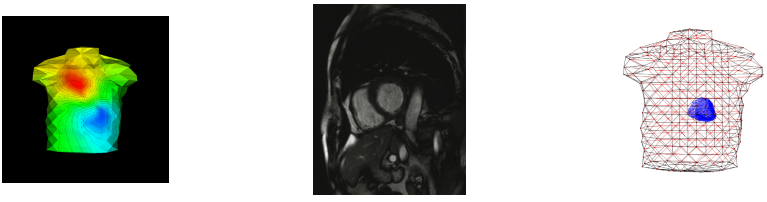

(a) (b)

Fig. 2. (a) Input patient data. Left: BSPM at 85ms of ventricular activation. Right: MRI slice. (b) Combined heart-torso model customized from patient-specific MRIs.

2.2 Volumetric Myocaridal TMP Imaging of MI

Experiment data. Fig 2 (a) lists paradigm inputs: MRI and BSP data collected from a patient with acute MI who returned for one-year follow-up MRI [7]. The set of static MRIs contains 9 slices, with 8mm inter-slice spacing and 1.33mm/pixel in-plane resolution. BSPs are recorded from 123 electrodes and interpolated to 370 nodes on the torso surface, each consisting of a single averaged PQRST complex sampled at 2k Hz. Anatomical locations of all electrodes and nodes are available. Reference MI interpretation is obtained from gadolinium enhanced images, evaluating the infarct extent (the percentage of infarcted myocardial mass), centroid (the myocardial segment containing the centroid) and segments containing infarcted tissues.

Model specification. For its ability to balance the model plausibility with inversion feasibility, the family of 2-variable FitzHugh-Nagumo-type models is favorable in IECG approaches. Among different variations, we select the model in [8] because it produces realistic TMP features which are closely related to BSP morphology. Besides, by a flexible control on TMP shapes, it allows an easy description of myocardial electrical heterogeneity and infarcted tissues.

Data processing. By segmenting MRIs slice by slice with hand-tracing, initial triangulated surfaces of thorax tissues are obtained. Because of the independent segmentation of each slice and the relatively low inter-slice imaging resolution, these surfaces are faceted. Surface smoothing is done by a two-stage Gaussian algorithm [9], which is able to reduce the shrinkage effect to keep the overall size and shape-feature of the surfaces. Fig 2 (b) displays the combined heart-torso model for the patient under study. The torso is assumed as a homogeneous conductor and represented with triangulated body surface. The 3D ventricular mass is described by a cloud of meshfree points [5]. Detailed 3D fiber structure is mapped from experimental results of [10] and determines intracellular conductive anisotropy. Transmural electrical heterogeneity is taken into account by associating different TMP shapes with epi-, endo-, and mid-myocardial regions [11] (Fig 3 (a)). In addition, to evaluate MI in a standard terminology, the LV wall is divided into 17 segments by AHA consensus [12] (Fig 3 (b)). Fig 4 displays the simulated normal TMP activation in the patient's ventricles.

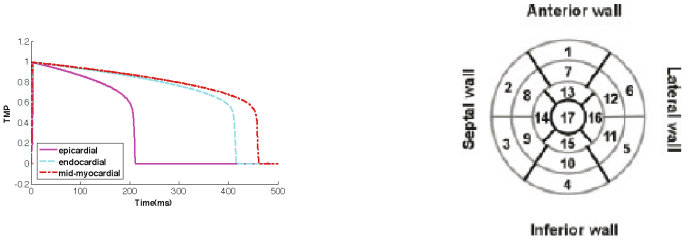

(a) (b)

Fig. 3. (a) Different TMP shapes in epi-, endo-, mid-myocardial tissues. (b) Schematics of the LV wall divided into 17 segments by AHA consensus (polar map) [12].

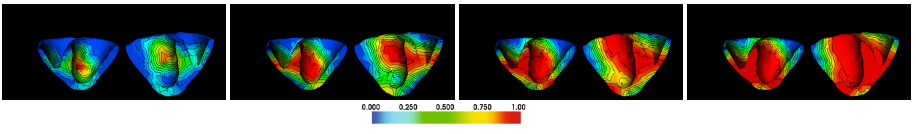

Fig. 4. Simulated normal TMP activation in the specific patient's ventricles. The color encodes TMP values and black contours represent potential ischrones. Left to Right: 35, 64, 78, 89ms after the onset of ventricular activation.

Meanwhile, preprocessing of patient BSP data is necessary to coordinate the real data with the physiological system. Firstly, since only *ventricular* electrical activity is considered at present, we select QRST intervals out of the complete BSP as paradigm input (Fig 5 (a)). Next, the TMP activity model has normalized TMP values, and its temporal interval for discretization is usually one magnitude smaller than BSP sampling interval. BSP data, therefore, go through temproal interpolation and magnitude scaling before being input into the paradigm.

TMP imaging and MI evaluation. In the following, we present a practical TMP imaging scheme composed of progressive iterations. Without using any prior knowledge of the infarct, TMP reconstruction starts with state estimation using models parameterized with standard values. The direct results of TMP estimates approximate local details of patient-specific volumetric cardiac arrhythmic pattern and arrhythmic substrates. Exploring a subset of the estimates, the infarct extent (EP), centroid (CE) and affected segments are evaluated. This approximate knowledge of the infarct is fed back to the paradigm to modify relevant model parameters and improve the 2nd-pass state estimation and MI evaluation. Subsequent passes of feedbacks and estimations iterate in a similar manner until no significant improvements are observed in the results.

Two primary characteristics of infarcted tissues are exhibited in the changes of activation time (AT) and TMP duration (PD), which can be calculated from TMP (Fig 5 (b)). The late AT and reduced PD of the estimates are used as the foremost indicator of infarct substrates. The relative label of AT ($rlAT$) is defined to represent the order in which the myocardium is activated and is

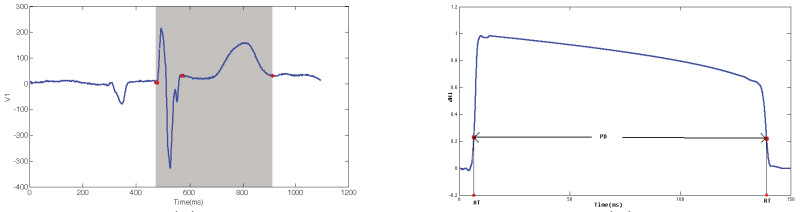

(a) (b)

Fig. 5. (a) Complete BSP signal and selected QRST interval (shadowed) used as paradigm inputs. (b) Calculation of AT and PD from TMP. AT is determined by the largest positive derivative, and repolarization time (RT) is when TMP value returns below that at AT. PD = RT − AT.

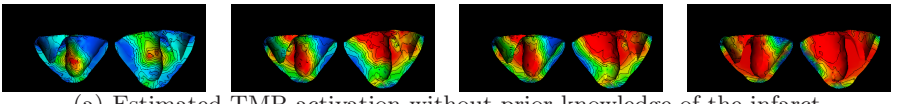

(a) Estimated TMP activation without prior knowledge of the infarct

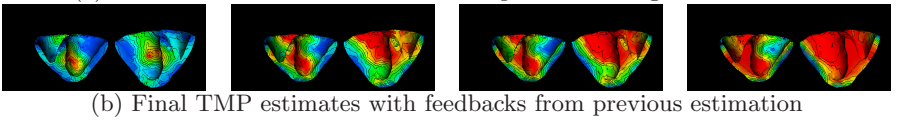

(b) Final TMP estimates with feedbacks from previous estimation

Fig. 6. Volumetric TMP imaging during ventricular activation. The color bar is the same as that in Fig 4. Left to Right: 35, 64, 78, 89ms after ventricular activation onset.

closer to 1 with larger AT. The relative label of PD ($rlPD$) is defined in a similar manner but $rlPD$ is closer to 1 with smaller PD. Infarcted tissues, therefore, would have $rlAT$ and $rlPD$ close to 1 in the estimates. Meanwhile, because the TMP activity model has impacts on the estimates, the discrepancy between model-generated and estimated $rlAT$ and $rlPD$ are used as the secondary infarct indicator and normalized into another two relative indices $rdAT$ and $rdPD$. Naturally, arrhythmogenic substrates would have larger $rdAT$ and/or $rdPD$. Accordingly, a relatively robust metric for infarct identification ($0 \leq M_i \leq 1$) is defined as the weighted summation of $rlAT, rlPD, rdAT$ and $rdPD$.

Generally, the distribution curve of M_i from all meshfree points shows a notable distinction between larger and smaller values. It provides a proper threshold T by which points with $M_i \geq T$ are initially suspected as infarcted. For each segment, the percentage of its suspected infarcted points (p) is calculated. Segments with $p \geq T_s$ and the containing suspected infarcted points are confirmed as infarcted, where T_s is another empirical threshold. By this step, isolated suspected infarcted points are removed. Since M_i actually measures the credibility of a meshfree point being infarcted, it is used to generate the approximate distribution map of the infarct substrate. EP is then calculated as the percentage of infarcted points in all ventricular meshfree points. CE is located as the center of infarcted points weighted by M_i. As we observed, exact values of weights and T, T_s have few impacts on CE localization or infarct identification. A set of empirical values for T, T_s

Table 1. Comparison of MI evaluation results with reference interpretation. SO is the segment overlap between the results and reference interpretation weighted by p.

	Reference Interpretation	Initial results	2nd-pass	3rd-pass
EP	52%	27%	27%	28%
SO	NA	70%	85%	90%
CE	10/11	12	11	11
segments	3-5,9-12,15-16	5-7,11-12,16	5,11-12,16	5,10-12,16

and weights of $rlAT, rdAT, rlPD, rdPD$ ($0.5, 30\%, 0.3, 0.2, 0.3, 0.2$) is used in our following analysis. Future studies would benefit from training or online adjustment of these parameters.

3 Results and Discussions

Results. Expert examinations report the infarct substrate as in inferior-lateral basal-middle LV. Announced as a challenge for MI evaluation, it attracted a variety of efforts [13,14,15]. The best results were obtained from simple ECG analysis without reference to MRIs [13]. The 4th and 5th place out of 6 awarded efforts took IECG approaches, based on aforementioned epicardial-potential-reconstruction [14] and heart-model-optimization [15] respectively. In the following, we will demonstrate the contribution of our paradigm to this problem.

TMP reconstruction starts by state estimation with standard models, and MI evaluation results at previous iteration are fed back to modify model parameters for the following TMP estimation. The results show negligible changes after 3 iterations. Fig 6 (a) lists the initial and final volumetric myocardial TMP estimates. Compared to the simulated normal TMP dynamics (Fig 4), both estimates exhibit distinct arrhythmic activation caused by conduction delay/block in the inferior-lateral basal-middle sections of LV. The final results further improves initial results by additional identification of the inferior infarct substrate.

Quantitative MI evaluation results for all iterations are listed in Table 1. The reference interpretation calculates EP in the segment level ($EP = 9/17 \simeq 52\%$). In comparison, able to differentiate between normal and infarcted tissues within the same segment, our approach usually produces smaller EP than the reference interpretation. Compared to the IECG efforts in the challenge [14,15], the initial results has the same 1-segment deviation in CE but EP and segments identification are largely improved. During the iteration, CE is corrected. EP and identification of affected segments are progressively refined, producing final results comparable to the best in the challenge [13]. The accuracy of TMP estimates is also validated by the closeness between estimates-generated BSPs and the input data (Fig 7). Derived from the final TMP estimates, the ventricular electrical activation time map (Fig 8) clearly indicates the infarct substrate with abnormally large AT. The associated distribution map of the infarct substrate (Fig 8 (b)) also localizes the substrate as around the inferior-lateral basal-middle

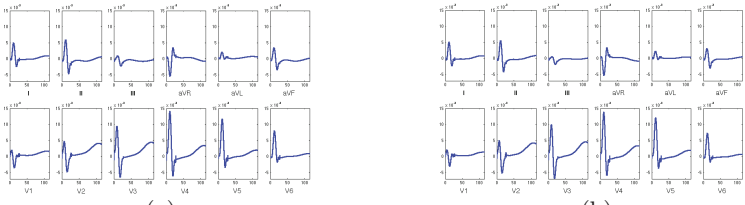

(a) (b)

Fig. 7. 12-lead ECG. (a): paradigm inputs (processed). (b): generated from final TMP estimates. They are in close accordance with relative root mean squared error as 0.15.

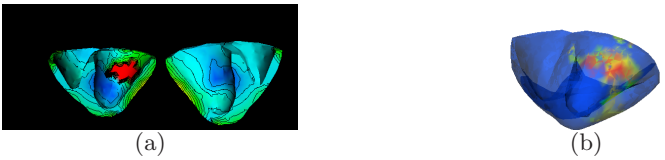

(a) (b)

Fig. 8. (a) Final ventricular electrical activation time map. The red and blue encodes maximum and minimum time values. Black contours represents time ischrones. (b) Final distribution map of infarct substrate (highlighted areas).

LV wall. In addition, instead of identifying the infarct substrate by segments, the distribution map displays its detailed location in the 3D myocardium.

Discussions. Without any prior knowledge of the infarct, this paradigm is able to produce MI evaluation results comparable to the best existent results [13]. More importantly, it has the advantage of describing complete volumetric myocardial TMP dynamics for the specific patient, from which MI evaluation only utilize a subset of information. When affirmative prior knowledge is unavailable, the presented progressive imaging scheme is practical. In practice, though, it is worthwhile to take advantage of prior knowledge from reliable sources, such as standard ECG diagnostic criteria and cardiac structural images.

In current study, the impact of model assumptions on the estimates are taken into account by considering the discrepancy between models and estimates during MI evaluation. An essential alternative is to reduce the constraining effects of models. By using unknown model parameters, simultaneous estimation of TMP and related myocardial electrophysiological property can modify models in accordance to patient data. Meanwhile, we have developed a data integration paradigm where information in BSPs and structural images are fused together for TMP imaging[16]. Its applicability will be investigated in the human study.

4 Conclusions

This human study demonstrates the potential of the presented paradigm as a noninvasive functional imaging technique for patient-specific volumetric cardiac

electrical activity. Its practical value is highlighted by the facts that 1), functional imaging of complete cardiac electrical activity is still a challenging task for current cardiac mapping techniques (noninvasive or invasive); 2), physiological modeling techniques, on the other hand, has the issue of requiring patient-specific knowledge *a prior*. The paradigm has the advantage to noninvasively describe volumetric patient-specific myocardial TMP dynamics. By exploring just a subset of the results, it shows promises in clinical practices such as MI evaluation.

Thorough validation of such technique is very challenging since it requires not only the collection of BSP and structural image of specific subjects, but also complete electrical mapping on the 3D myocardium. The dataset provided in current case is valuable for reasonable validations. In the future, it is desirable to look into the possibility of obtaining 3D cardiac electrical mapping data, and more real-data studies will be performed with regard to various pathologies.

References

1. Mirvis, D.M.: What's wrong with electrocardiography? J. Electrocardiol 31, 313–316 (1998)
2. Kornreich, F., Montague, T.J., Rautaharju, P.M.: Identification of first acute q wave and non-q wave myocardial infarction by multivariate analysis of body surface potential maps. Circ. 84, 2442–2453 (1991)
3. Burnes, J.E., Rudy, Y.: Noninvasive ecg imaging of electrophysiologically abnormal substrates in infarcted hearts: a model study. Circ. 101, 533–540 (2000)
4. Li, G., He, B.: Noninvasive estimatin of myocardial infarction by means of a heart-model-based imaging approach: a simulation study. Med. Biol. Eng. Comput. 42, 128–136 (2004)
5. Wang, L., Zhang, H., Liu, H., Shi, P.: Imaging of 3D cardiac electrical activity: A model-based recovery framework. In: Larsen, R., Nielsen, M., Sporring, J. (eds.) MICCAI 2006. LNCS, vol. 4190, pp. 792–799. Springer, Heidelberg (2006)
6. Wang, L., Zhang, H., Shi, P.: Towards noninvasive 3D imaging of cardiac arrhythmias. In: Sachse, F.B., Seemann, G. (eds.) FIHM 2007. LNCS, vol. 4466, pp. 280–289. Springer, Heidelberg (2007)
7. Goldberger, A.L., et al.: Physiobank, physiotoolkit, and physionet components of a new research resource for complex physiological signals. Cric. 101, 215–220 (2000)
8. Aliev, R.R., Panfilov, A.V.: A simple two-variable model of cardiac excitation. Chaos, Solitions & Fractals 7(3), 293–301 (1996)
9. Taubin, G.: Curve and surface smoothing without shrinkage. In: Proc. ICCV, pp. 825–857 (1995)
10. Nash, M.: Mechanics and Material Properties of the Heart using an Anatomically Accurate Mathematical Model. PhD thesis, Univ. of Auckland, New Zealand (May 1998)
11. Yan, G.X., et al.: Charactertistics and distribution of m cells in arterially perfused canine left ventricular wedge preparations. Circ. 98, 1921–1927 (1998)
12. Cerqueira, M.D., et al.: Standardized myocardial segmentation and nomenclature for tomographic imaging of the heart. Circ. 105, 539–542 (2002)

13. Mneimneh, M.A., Povinelli, R.J.: Rps/gmm approach toward the localization of myocardial infarction. In: Proc. CinC. (2007)
14. Dawoud, F.D.: Using inverse electrocardiography to image myocardial infarction. In: Proc. CinC. (2007)
15. Farina, D.: Model-based approach to the localization of infarction. In: Proc. CinC. (2007)
16. Wang, L., Zhang, H., Wong, K.C., Shi, P.: Idynamic structural-image-guided non-invasive 3d cardiac electrophysiological mapping. In: Proc. ICIP (in press, 2008)